

1  
2  
3  
4  
5  
6  
7  
8  
9  
10  
11  
12  
13  
14  
15  
16  
17  
18  
19  
20  
21  
22  
23  
24  
25  
26  
27  
28  
29  
30  
31  
32

*Manuscript*

## **Characterizing a thermostable Cas9 for bacterial genome editing and silencing**

Ioannis Mougias<sup>1\*</sup>, Prarthana Mohanraju<sup>1\*</sup>, Elleke F. Bosma<sup>1‡\*</sup>,  
Valentijn Vrouwe<sup>1</sup>, Max Finger Bou<sup>1</sup>, Mihris I. S. Naduthodi<sup>1</sup>, Alexander Gussak<sup>1</sup>,  
Rudolf B. L. Brinkman<sup>2</sup>, Richard van Kranenburg<sup>1, 2</sup>, John van der Oost<sup>1†</sup>

<sup>1</sup>Laboratory of Microbiology, Wageningen University, Stippeneng 4, 6708 WE Wageningen, The Netherlands

<sup>2</sup>Corbion, Arkelsedijk 46, 4206 AC Gorinchem, The Netherlands

<sup>‡</sup>Present address: The Novo Nordisk Foundation Center for Biosustainability, Technical University of Denmark, Kemitorvet B220, 2800 Kgs. Lyngby, Denmark

\*These authors contributed equally to this work.

†To whom correspondence should be addressed: J.v.d.O. ([john.vanderoost@wur.nl](mailto:john.vanderoost@wur.nl))

33 **Abstract**

34 **CRISPR-Cas9 based genome engineering tools have revolutionized fundamental research**  
35 **and biotechnological exploitation of both eukaryotes and prokaryotes. However, the**  
36 **mesophilic nature of the established Cas9 systems does not allow for applications that**  
37 **require enhanced stability, including engineering at elevated temperatures. Here, we**  
38 **identify and characterize ThermoCas9: an RNA-guided DNA-endonuclease from the**  
39 **thermophilic bacterium *Geobacillus thermodenitrificans* T12. We show that ThermoCas9**  
40 **is active *in vitro* between 20°C and 70°C, a temperature range much broader than that of**  
41 **the currently used Cas9 orthologues. Additionally, we demonstrate that ThermoCas9**  
42 **activity at elevated temperatures is strongly associated with the structure of the employed**  
43 **sgRNA. Subsequently, we develop ThermoCas9-based engineering tools for gene deletion**  
44 **and transcriptional silencing at 55°C in *Bacillus smithii* and for gene deletion at 37°C in**  
45 ***Pseudomonas putida*. Altogether, our findings provide fundamental insights into a**  
46 **thermophilic CRISPR-Cas family member and establish the first Cas9-based bacterial**  
47 **genome editing and silencing tool with a broad temperature range.**

## 48 **Introduction**

49 Clustered Regularly Interspaced Short Palindromic Repeats (CRISPR) and the CRISPR-  
50 associated (Cas) proteins provide adaptive and heritable immunity in prokaryotes against  
51 invading genetic elements<sup>1-4</sup>. CRISPR-Cas systems are subdivided into two classes (1 and 2)  
52 and six types (I-VI), depending on their complexity and signature proteins<sup>5</sup>. Class 2 systems,  
53 including type-II CRISPR-Cas9 and type V CRISPR-Cas12a (previously called CRISPR-  
54 Cpf1) have recently been exploited as genome engineering tools for both eukaryotes<sup>6-10</sup> and  
55 prokaryotes<sup>11-13</sup>. These systems are among the simplest CRISPR-Cas systems known as they  
56 introduce targeted double stranded DNA breaks (DSBs) based on a ribonucleoprotein (RNP)  
57 complex formed by a single Cas endonuclease and an RNA guide.

58 The guide of Cas9 consists of a crRNA (CRISPR RNA):tracrRNA (trans-activating-  
59 CRISPR-RNA) duplex. For engineering purposes, the crRNA:tracrRNA duplex has been  
60 simplified by generating a chimeric, single guide RNA (sgRNA) to guide Cas9 upon co-  
61 expression<sup>14</sup>. In addition, cleavage of the target DNA requires a protospacer adjacent motif  
62 (PAM): a 3-8 nucleotide (nt) long sequence located next to the targeted protospacer that is  
63 highly variable between different Cas9 proteins<sup>15-17</sup>. Cas9 endonucleases contain two catalytic  
64 domains, denoted as RuvC and HNH. Substituting catalytic residues in one of these domains  
65 results in Cas9 nickase variants, and in both domains in an inactive variant<sup>18-20</sup>. The inactive or  
66 dead Cas9 (dCas9) has been instrumental as an efficient gene silencing system and for  
67 modulating the expression of essential genes<sup>11,21,22</sup>.

68 To date, *Streptococcus pyogenes* Cas9 (SpCas9) is the best characterized and most widely  
69 employed Cas9 for genome engineering. Although a few other type-II systems have been  
70 exploited for bacterial genome engineering purposes, none of them is derived from a  
71 thermophilic organism<sup>23</sup>. Characterization of such CRISPR-Cas systems would be interesting  
72 to gain fundamental insights as well as to develop novel applications.

73 Although basic genetic tools are available for a number of thermophiles<sup>24-27</sup>, the efficiency  
74 of these tools is still too low to enable full exploration and exploitation of this interesting group  
75 of organisms. Based on our finding that SpCas9 is not active *in vivo* at or above 42°C, we have  
76 previously developed a SpCas9-based engineering tool for facultative thermophiles, combining  
77 homologous recombination at elevated temperatures and SpCas9-based counter-selection at  
78 moderate temperatures<sup>28</sup>. However, a Cas9-based editing and silencing tool for obligate  
79 thermophiles is not yet available as SpCas9 is not active at elevated temperatures<sup>28,29</sup>, and to  
80 date no thermophilic Cas9 has been adapted for such purpose. Here, we describe the  
81 characterization of ThermoCas9: an RNA-guided DNA-endonuclease from the CRISPR-Cas

82 type-IIc system of the thermophilic bacterium *Geobacillus thermodenitrificans* T12<sup>30</sup>. We  
83 show that ThermoCas9 is active *in vitro* between 20 and 70°C and demonstrate the effect of the  
84 sgRNA-structure on its thermostability. We apply ThermoCas9 for *in vivo* genome editing and  
85 silencing of the industrially important thermophile *Bacillus smithii* ET 138<sup>31</sup> at 55°C, creating  
86 the first Cas9-based genome engineering tool readily applicable to thermophiles. In addition,  
87 we apply ThermoCas9 for *in vivo* genome editing of the mesophile *Pseudomonas putida*  
88 KT2440, for which to date no CRISPR-Cas9-based editing tool had been described<sup>32,33</sup>,  
89 confirming the wide temperature range and broad applicability of this novel Cas9 system.

90

## 91 **Results**

### 92 **ThermoCas9 identification and purification**

93 We recently isolated and sequenced *Geobacillus thermodenitrificans* strain T12, a Gram  
94 positive, thermophilic bacterium with an optimal growth temperature at 65°C<sup>30</sup>. Contrary to  
95 previous claims that type II CRISPR-Cas systems are not present in thermophilic bacteria<sup>34</sup>, the  
96 sequencing results revealed the existence of a type-IIc CRISPR-Cas system in the genome of  
97 *G. thermodenitrificans* T12 (Figure 1A). The Cas9 endonuclease of this system (ThermoCas9)  
98 was predicted to be relatively small (1082 amino acids) compared to other Cas9 orthologues,  
99 such as SpCas9 (1368 amino acids). The size difference is mostly due to a truncated REC lobe,  
100 as has been demonstrated for other small Cas9 orthologues (Supplementary Fig. 1)<sup>35</sup>.  
101 Furthermore, ThermoCas9 was expected to be active at least around the temperature optimum  
102 of *G. thermodenitrificans* T12<sup>30</sup>. Using the ThermoCas9 sequence as query, we performed  
103 BLAST-P searches in the NCBI/non-redundant protein sequences dataset, and found a number  
104 of highly identical Cas9 orthologues (87-99% identity at amino acid level, Supplementary Table  
105 1), mostly within the *Geobacillus* genus, supporting the idea that ThermoCas9 is part of a highly  
106 conserved defense system of thermophilic bacteria (Figure 1B). These characteristics suggested  
107 it may be a potential candidate for exploitation as a genome editing and silencing tool for  
108 thermophilic microorganisms, and for conditions at which enhanced protein robustness is  
109 required.

110 We initially performed *in silico* prediction of the crRNA and tracrRNA modules of the *G.*  
111 *thermodenitrificans* T12 CRISPR-Cas system using a previously described approach<sup>11,35</sup>. Based  
112 on this prediction, a 190 nt sgRNA chimera was designed by linking the predicted full-size  
113 crRNA (30 nt long spacer followed by 36 nt long repeat) and tracrRNA (36 nt long anti-repeat

114 followed by a 88 nt sequence with three predicted hairpin structures). ThermoCas9 was  
115 heterologously expressed in *E. coli* and purified to homogeneity. Hypothesizing that the loading  
116 of the sgRNA to the ThermoCas9 would stabilize the protein, we incubated purified apo-  
117 ThermoCas9 and ThermoCas9 loaded with *in vitro* transcribed sgRNA at 60°C and 65°C, for  
118 15 and 30 min. SDS-PAGE analysis showed that the purified ThermoCas9 denatures at 65°C  
119 but not at 60°C, while the denaturation temperature of ThermoCas9-sgRNA complex is above  
120 65°C (Figure 1C). The demonstrated thermostability of ThermoCas9 implied its potential as a  
121 thermo-tolerant CRISPR-Cas9 genome editing tool, and encouraged us to analyze some  
122 relevant molecular features in more detail.

### 123 **ThermoCas9 PAM determination**

124 The first step towards the characterization of ThermoCas9 was the *in silico* prediction of its  
125 PAM preferences for successful cleavage of a DNA target. We used the 10 spacers of the *G.*  
126 *thermodenitrificans* T12 CRISPR locus to search for potential protospacers in viral and plasmid  
127 sequences using CRISPRtarget<sup>36</sup>. As only two hits were obtained with phage genomes  
128 (Supplementary Fig. 2A), it was decided to proceed with an *in vitro* PAM determination  
129 approach. The predicted sgRNA sequence was generated by *in vitro* transcription, including a  
130 spacer that should allow for ThermoCas9-based targeting of linear dsDNA substrates with a  
131 matching protospacer. The protospacer was flanked at its 3'-end by randomized 7-base pair  
132 (bp) sequences. After performing ThermoCas9-based cleavage assays at 55°C, the cleaved  
133 sequences of the library (together with a non-targeted library sample as control) were separated  
134 from uncleaved sequences, by gel electrophoresis, and analyzed by deep-sequencing in order  
135 to identify the ThermoCas9 PAM preference (Figure 2A). The sequencing results revealed that  
136 ThermoCas9 introduces double stranded DNA breaks that, in analogy with the mesophilic Cas9  
137 variants, are located mostly between the 3<sup>rd</sup> and the 4<sup>th</sup> PAM proximal nucleotides, at the 3' end  
138 of the protospacer. Moreover, the cleaved sequences revealed that ThermoCas9 recognizes a  
139 5'-NNN<sup>1</sup>CNR-3' PAM, with subtle preference for cytosine at the 1<sup>st</sup>, 3<sup>rd</sup>, 4<sup>th</sup> and 6<sup>th</sup> PAM  
140 positions (Figure 2B). Recent studies have revealed the importance of the 8<sup>th</sup> PAM position for  
141 target recognition of some Type IIC Cas9 orthologues<sup>17,37</sup>. For this purpose, and taking into  
142 account the results from the *in silico* ThermoCas9 PAM prediction (Supplementary Fig. 2), we  
143 performed additional PAM determination assays. This revealed optimal targeting efficiency in  
144 the presence of an adenine at the 8<sup>th</sup> PAM position (Figure 2C). Interestingly, despite the limited  
145 number of hits, the aforementioned *in silico* PAM prediction (Supplementary Fig. 2B) also  
146 suggested the significance of a cytosine at the 5<sup>th</sup> and an adenine at the 8<sup>th</sup> PAM positions.

147 To further clarify the ambiguity of the PAM at the 6<sup>th</sup> and 7<sup>th</sup> PAM positions, we generated  
148 a set of 16 different target DNA fragments in which the matching protospacer was flanked by  
149 5'-CCCCNNA-3' PAMs. Cleavage assays of these fragments (each with a unique combination  
150 of the 6<sup>th</sup> and 7<sup>th</sup> nucleotide) were performed in which the different components (ThermoCas9,  
151 sgRNA guide, dsDNA target) were pre-heated separately at different temperatures (20, 30, 37,  
152 45, 55 and 60°C) for 10 min before combining and incubating them for 1 hour at the  
153 corresponding assay temperature. When the assays were performed at temperatures between  
154 37°C and 60°C, all the different DNA substrates were cleaved (Figure 2D, S3). However, the  
155 most digested target fragments consisted of PAM sequences (5<sup>th</sup> to 8<sup>th</sup> PAM positions) 5'-  
156 CNA-3' and 5'-CMCA-3', whereas the least digested targets contained a 5'-CAKA-3' PAM.  
157 At 30°C, only cleavage of the DNA substrates with the optimal PAM sequences (5<sup>th</sup> to 8<sup>th</sup> PAM  
158 positions) 5'-CNA-3' and 5'-CMCA-3' was observed (Figure 2D). Lastly, at 20°C only the  
159 DNA substrates with (5<sup>th</sup> to 8<sup>th</sup> PAM positions) 5'-CVAA-3' and 5'-CCCA-3' PAM sequences  
160 were targeted (Supplementary Fig. 3), making these sequences the most preferred PAMs. Our  
161 findings demonstrate that at its lower temperature limit, ThermoCas9 only cleaves fragments  
162 with a preferred PAM. This characteristic could be exploited during *in vivo* editing processes,  
163 for example to avoid off-target effects in eukaryotic Cas9-based genome editing.

#### 164 **Metal ion dependency, thermostability and truncations**

165 Previously characterized, mesophilic Cas9 endonucleases employ divalent cations to  
166 catalyze the generation of DSBs in target DNA<sup>14,38</sup>. To determine the ion dependency of  
167 ThermoCas9 cleavage activity, plasmid cleavage assays were performed in the presence of one  
168 of the following divalent cations: Mg<sup>2+</sup>, Ca<sup>2+</sup>, Mn<sup>2+</sup>, Fe<sup>2+</sup>, Co<sup>2+</sup>, Ni<sup>2+</sup>, and Zn<sup>2+</sup>; an assay with  
169 the cation-chelating agent EDTA was included as negative control. As expected, target dsDNA  
170 was cleaved in the presence of divalent cations and remained intact in the presence of EDTA  
171 (Supplementary Fig. 5A). The DNA cleavage activity of ThermoCas9 was the highest when  
172 Mg<sup>2+</sup> and Mn<sup>2+</sup> was added to the reaction consistent with other Cas9 variants<sup>14,20,39</sup>. Addition  
173 of Fe<sup>2+</sup>, Co<sup>2+</sup>, Ni<sup>2+</sup>, or Zn<sup>2+</sup> ions also mediated cleavage. Ca<sup>2+</sup> only supported plasmid nicking,  
174 suggesting that with this cation only one of the endonuclease domains is functional.

175 The predicted tracrRNA consists of the anti-repeat region followed by three hairpin  
176 structures (Figure 3A). Using the tracrRNA along with the crRNA to form a sgRNA chimera  
177 resulted in successful guided cleavage of the DNA substrate. It was observed that a 41-nt long  
178 deletion of the spacer distal end of the full-length repeat-anti-repeat hairpin (Figure 3A), most  
179 likely better resembling the dual guide's native state, had little to no effect on the DNA cleavage

180 efficiency. The effect of further truncation of the predicted hairpins (Figure 3A) on the cleavage  
181 efficiency of ThermoCas9 was evaluated by performing a cleavage time-series in which all the  
182 components (sgRNA, ThermoCas9, substrate DNA) were pre-heated separately at different  
183 temperatures (37-65°C) for 1, 2 and 5 min before combining and incubating them for 1 hour at  
184 various assay temperatures (37-65°C). The number of predicted stem-loops of the tracrRNA  
185 scaffold seemed to play a crucial role in DNA cleavage; when all three loops were present, the  
186 cleavage efficiency was the highest at all tested temperatures, whereas the efficiency decreased  
187 upon removal of the 3' hairpin (Figure 3B). Moreover, the cleavage efficiency drastically  
188 dropped upon removal of both the middle and the 3' hairpins (Supplementary Fig. 4). Whereas  
189 pre-heating ThermoCas9 at 65°C for 1 or 2 min resulted in detectable cleavage, the cleavage  
190 activity was abolished after 5 min incubation. The thermostability assay showed that sgRNA  
191 variants without the 3' stem-loop result in decreased stability of the ThermoCas9 protein at  
192 65°C, indicating that a full length tracrRNA is required for optimal ThermoCas9-based DNA  
193 cleavage at elevated temperatures. Additionally, we also varied the lengths of the spacer  
194 sequence (from 25 to 18 nt) and found that spacer lengths of 23, 21, 20 and 19 cleaved the  
195 targets with the highest efficiency. The cleavage efficiency drops significantly when a spacer  
196 of 18 nt is used.

197 *In vivo*, the ThermoCas9:sgRNA RNP complex is probably formed within seconds.  
198 Together with the above findings, this motivated us to evaluate the activity and thermostability  
199 of the RNP. Pre-assembled RNP complex was heated at 60, 65 and 70°C for 5 and 10 min  
200 before adding pre-heated DNA and subsequent incubation for 1 hour at 60, 65 and 70°C.  
201 Strikingly, we observed that the ThermoCas9 RNP was active up to 70°C, in spite of its pre-  
202 heating for 5 min at 70°C (Figure 3C). This finding confirmed our assumption that the  
203 ThermoCas9 stability strongly correlates with the association of an appropriate sgRNA guide<sup>40</sup>.

204 Proteins of thermophilic origin generally retain activity at lower temperatures. Hence, we  
205 set out to compare the ThermoCas9 temperature range to that of the *Streptococcus pyogenes*  
206 Cas9 (SpCas9). Both Cas9 homologues were subjected to *in vitro* activity assays between 20  
207 and 65°C. Both proteins were incubated for 5 min at the corresponding assay temperature prior  
208 to the addition of the sgRNA and the target DNA molecules. In agreement with previous  
209 analysis<sup>28,29</sup>, the mesophilic SpCas9 was inactive above 45°C (Figure 3D); above this  
210 temperature SpCas9 activity rapidly decreased to undetectable levels. In contrast, ThermoCas9  
211 cleavage activity could be detected between 25 and 65°C (Figure 3D). This indicates the

212 potential to use ThermoCas9 as a genome editing tool for both thermophilic and mesophilic  
213 organisms.

214 Based on previous reports that certain type-IIIC systems were efficient single stranded DNA  
215 cutters<sup>40,39</sup>, we tested the activity of ThermoCas9 on ssDNA substrates. However, no cleavage  
216 was observed, indicating that ThermoCas9 is a dsDNA nuclease (Supplementary Fig. 5B).

### 217 **ThermoCas9-based gene deletion in the thermophile *B. smithii***

218 We set out to develop a ThermoCas9-based genome editing tool for thermophilic bacteria.  
219 This group of bacteria is of great interest both from a fundamental as well as from an applied  
220 perspective. For biotechnological applications, their thermophilic nature results in for example  
221 less cooling costs, higher reaction rates and less contamination risk compared to the widely  
222 used mesophilic industrial work horses such as *E. coli*<sup>24,25,41,42</sup>. Here, we show a proof of  
223 principle study on the use of ThermoCas9 as genome editing tool for thermophiles, employing  
224 *Bacillus smithii* ET 138 cultured at 55°C. Its wide substrate utilization range, thermophilic and  
225 facultative anaerobic nature, combined with its genetic amenability make this an organism with  
226 high potential as platform organism for the production of green chemicals in a  
227 biorefinery<sup>24,28,31,43</sup>. In order to use a minimum of genetic parts, we followed a single plasmid  
228 approach. We constructed a set of pNW33n-based pThermoCas9 plasmids containing the  
229 *thermocas9* gene under the control of the native *xylL* promoter ( $P_{xylL}$ ), a homologous  
230 recombination template for repairing Cas9-induced double stranded DNA breaks within a gene  
231 of interest, and a sgRNA expressing module under control of the constitutive *pta* promoter ( $P_{pta}$ )  
232 from *Bacillus coagulans* (Figure 4A).

233 The first goal was the deletion of the full length *pyrF* gene from the genome of *B. smithii*  
234 ET 138. The pNW33n-derived plasmids pThermoCas9\_bs $\Delta$ pyrF1 and  
235 pThermoCas9\_bs $\Delta$ pyrF2 were used for expression of different ThermoCas9 guides with  
236 spacers targeting different sites of the *pyrF* gene, while a third plasmid (pThermoCas9\_ctrl)  
237 contained a random non-targeting spacer in the sgRNA expressing module. Transformation of  
238 *B. smithii* ET 138 competent cells at 55°C with the control plasmids pNW33n (no guide) and  
239 pThermoCas9\_ctrl resulted in the formation of ~200 colonies each. Out of 10 screened  
240 pThermoCas9\_ctrl colonies, none contained the  $\Delta$ *pyrF* genotype, confirming findings from  
241 previous studies that, in the absence of appropriate counter-selection, homologous  
242 recombination in *B. smithii* ET 138 is not sufficient to obtain clean mutants<sup>28,43</sup>. In contrast,  
243 transformation with the pThermoCas9\_bs $\Delta$ pyrF1 and pThermoCas9\_bs $\Delta$ pyrF2 plasmids



244 resulted in 20 and 0 colonies respectively. Out of the ten pThermoCas9\_ΔpyrF1 colonies  
245 screened, one was a clean ΔpyrF mutant whereas the rest had a mixed wild type/ΔpyrF  
246 genotype (Figure 4B), proving the applicability of the system, as the designed homology  
247 directed repair of the targeted *pyrF* gene was successful. Contrary to eukaryotes, most  
248 prokaryotes including *B. smithii* do not possess a functional NHEJ system, and hence DSBs  
249 induced by Cas9 have been shown to be lethal in the absence of a functional HR system and/or  
250 of an appropriate HR template<sup>11,28</sup>. Hence, Cas9 functions as stringent counter-selection system  
251 to kill cells that have not performed the desired HR prior to or post Cas9 cleavage<sup>11,28,44</sup>. The  
252 combination of lack of NHEJ and low HR-frequencies found in most prokaryotes provides the  
253 basis for the power of Cas9-based editing but also creates the need for tight control of Cas9  
254 activity<sup>11,28,44</sup>. As the promoter we use here for *thermocas9*-expression is not sufficiently  
255 controllable and HR is inefficient in *B. smithii*<sup>28,43</sup>, the low number (pyrF1) or even complete  
256 lack (pyrF2) of colonies we observed here in the presence of an HR template confirms the high  
257 *in vivo* activity of ThermoCas9 at 55°C. In the SpCas9-based counter-selection system we  
258 previously developed for *B. smithii*, the activity of Cas9 was very tightly controlled by the  
259 growth temperature rather than by gene expression. This allowed for extended time for the cells  
260 to perform HR prior to Cas9 counter-selection, resulting in a higher *pyrF* deletion efficiency<sup>28</sup>.  
261 We anticipate that the use of a tightly controlled promoter will increase efficiencies of the  
262 ThermoCas9-system.

### 263 **ThermoCas9-based gene deletion in the mesophile *P. putida***

264 To broaden the applicability of the ThermoCas9-based genome editing tool and to evaluate  
265 whether our *in vitro* results could be confirmed *in vivo*, we next evaluated its activity in the  
266 mesophilic Gram-negative bacterium *P. putida* KT2440. This soil bacterium is well-known for  
267 its unusual metabolism and biodegradation capacities, especially of aromatic compounds.  
268 Recently, interest in this organism has further increased due to its potential as platform host for  
269 biotechnology purposes using metabolic engineering<sup>45,46</sup>. However, to date no CRISPR-Cas9-  
270 based editing system has been reported for *P. putida* whereas such a system would greatly  
271 increase engineering efficiencies and enhance further study and use of this organism<sup>32,33</sup>. Once  
272 more, we followed a single plasmid approach and combined homologous recombination and  
273 ThermoCas9-based counter-selection. We constructed the pEMG-based  
274 pThermoCas9\_ppΔpyrF plasmid containing the *thermocas9* gene under the control of the 3-  
275 methylbenzoate-inducible Pm-promoter, a homologous recombination template for deletion of  
276 the *pyrF* gene and a sgRNA expressing module under the control of the constitutive P3

277 promoter. After transformation of *P. putida* KT2440 cells and PCR confirmation of plasmid  
278 integration, a colony was inoculated in selective liquid medium for overnight culturing at 37°C.  
279 The overnight culture was used for inoculation of selective medium and ThermoCas9  
280 expression was induced with 3-methylbenzoate. Subsequently, dilutions were plated on non-  
281 selective medium, supplemented with 3-methylbenzoate. For comparison, we performed a  
282 parallel experiment without inducing ThermoCas9 expression with 3-methylbenzoate. The  
283 process resulted in 76 colonies for the induced culture and 52 colonies for the non-induced  
284 control culture. For the induced culture, 38 colonies (50%) had a clean deletion genotype and  
285 6 colonies had mixed wild-type/deletion genotype. On the contrary, only 1 colony (2%) of the  
286 non-induced culture had the deletion genotype and there were no colonies with mixed wild-  
287 type/deletion genotype retrieved (Supplementary Fig. 6). These results show that ThermoCas9  
288 can be used as an efficient counter-selection tool in the mesophile *P. putida* KT2440 when  
289 grown at 37°C.

### 290 **ThermoCas9-based gene silencing**

291 An efficient thermoactive transcriptional silencing CRISPRi tool is currently not available.  
292 Such a system could greatly facilitate metabolic studies of thermophiles. A catalytically dead  
293 variant of ThermoCas9 could serve this purpose by steadily binding to DNA elements without  
294 introducing dsDNA breaks. To this end, we identified the RuvC and HNH catalytic domains of  
295 ThermoCas9 and introduced the corresponding D8A and H582A mutations for creating a dead  
296 (d) ThermoCas9. After confirmation of the designed sequence, ThermodCas9 was  
297 heterologously produced, purified and used for an *in vitro* cleavage assay with the same DNA  
298 target as used in the aforementioned ThermoCas9 assays; no cleavage was observed confirming  
299 the catalytic inactivation of the nuclease.

300 Towards the development of a ThermodCas9-based CRISPRi tool, we aimed for the  
301 transcriptional silencing of the highly expressed *ldhL* gene from the genome of *B. smithii* ET  
302 138. We constructed the pNW33n-based vectors pThermoCas9i\_ *ldhL* and pThermoCas9i\_ctrl.  
303 Both vectors contained the *thermodCas9* gene under the control of P<sub>xytL</sub> promoter and a sgRNA  
304 expressing module under the control of the constitutive P<sub>pta</sub> promoter (Figure 4C). The  
305 pThermoCas9i\_ *ldhL* plasmid contained a spacer for targeting the non-template DNA strand at  
306 the 5' end of the 138 *ldhL* gene in *B. smithii* ET 138 (Supplementary Fig. 7). The position and  
307 targeted strand selection were based on previous studies<sup>18,47</sup>, aiming for the efficient down-  
308 regulation of the *ldhL* gene. The pThermoCas9i\_ctrl plasmid contained a random non-targeting  
309 spacer in the sgRNA-expressing module. The constructs were used to transform *B. smithii* ET

310 138 competent cells at 55°C followed by plating on LB2 agar plates, resulting in equal amounts  
311 of colonies. Two out of the approximately 700 colonies per construct were selected for culturing  
312 under microaerobic lactate-producing conditions for 24 hours, as described previously<sup>31</sup>. The  
313 growth of the pThermoCas9i\_ *ldhL* cultures was 50% less than the growth of the  
314 pThermoCas9i\_ctrl cultures (Figure 4E). We have previously shown that deletion of the *ldhL*  
315 gene leads to severe growth retardation in *B. smithii* ET 138 due to a lack of Ldh-based NAD<sup>+</sup>-  
316 regenerating capacity under micro-aerobic conditions<sup>43</sup>. Thus, the observed decrease in growth  
317 is likely caused by the transcriptional inhibition of the *ldhL* gene and subsequent redox  
318 imbalance due to loss of NAD<sup>+</sup>-regenerating capacity. Indeed, HPLC analysis revealed 40%  
319 reduction in lactate production of the *ldhL* silenced cultures, and RT-qPCR analysis showed  
320 that the transcription levels of the *ldhL* gene were significantly reduced in the  
321 pThermoCas9i\_ *ldhL* cultures compared to the pThermoCas9i\_ctrl cultures (Figure 4E).

322

## 323 Discussion

324 Most CRISPR-Cas applications are based on RNA-guided DNA interference by Class 2  
325 CRISPR-Cas proteins, such as Cas9 and Cas12a<sup>6-13</sup>. Prior to this work, there were only a few  
326 examples of Class 1 CRISPR-Cas systems present in thermophilic bacteria and archaea<sup>5,48</sup>,  
327 which have been used for genome editing of thermophiles<sup>34</sup>. As a result, the application of  
328 CRISPR-Cas technologies was mainly restricted to temperatures below 42°C, due to the  
329 mesophilic nature of the employed Cas-endonucleases<sup>28,29</sup>. Hence, this has excluded application  
330 of these technologies in obligate thermophiles and in experimental approaches that require  
331 elevated temperatures and/or improved protein stability.

332 In the present study, we have characterized ThermoCas9, a Cas9 orthologue from the  
333 thermophilic bacterium *G. thermodenitrificans* T12, a strain that we previously isolated from  
334 compost<sup>30</sup>. Data mining revealed additional Cas9 orthologues in the genomes of other  
335 thermophiles, which were nearly identical to ThermoCas9, showing that CRISPR-Cas type II  
336 systems do exist in thermophiles, at least in some branches of the *Bacillus* and *Geobacillus*  
337 genera. We showed that ThermoCas9 is active *in vitro* in a wide temperature range of 20-70°C,  
338 which is much broader than the range of its mesophilic orthologue SpCas9. The extended  
339 activity and stability of ThermoCas9 allows for its application in molecular biology techniques  
340 that require DNA manipulation at temperatures of 20-70°C, as well as its exploitation in harsh  
341 environments that require robust enzymatic activity. Furthermore, we identified several factors

342 that are important for conferring the thermostability of ThermoCas9. Firstly, we showed that  
343 the PAM preferences of ThermoCas9 are very strict for activity in the lower part of the  
344 temperature range ( $\leq 30^{\circ}\text{C}$ ), whereas more variety in the PAM is allowed for activity at the  
345 moderate to optimal temperatures ( $37\text{-}60^{\circ}\text{C}$ ). Secondly, we showed that ThermoCas9 activity  
346 and thermostability strongly depends on the association with an appropriate sgRNA guide. This  
347 stabilization of the multi-domain Cas9 protein is most likely the result of a major  
348 conformational change from an open/flexible state to a rather compact state, as described for  
349 SpCas9 upon guide binding<sup>49</sup>.

350 Based on the here described characterization of the novel ThermoCas9, we successfully  
351 developed genome engineering tools for strictly thermophilic prokaryotes. We showed that  
352 ThermoCas9 is active *in vivo* at  $55^{\circ}\text{C}$  and  $37^{\circ}\text{C}$ , and we adapted the current Cas9-based  
353 engineering technologies for the thermophile *B. smithii* ET 138 and the mesophile *P. putida*  
354 KT2440. Due to the wide temperature range of ThermoCas9, it is anticipated that the simple,  
355 effective and single plasmid-based ThermoCas9 approach will be suitable for a wide range of  
356 thermophilic and mesophilic microorganisms that can grow at temperatures from  $37^{\circ}\text{C}$  up to  
357  $70^{\circ}\text{C}$ . This complements the existing mesophilic technologies, allowing their use for a large  
358 group of organisms for which these efficient tools were thus far unavailable

359 Screening natural resources for novel enzymes with desired traits is unquestionably  
360 valuable. Previous studies have suggested that the adaptation of a mesophilic Cas9 orthologue  
361 to higher temperatures, with directed evolution and protein engineering, would be the best  
362 approach towards the construction of a thermophilic Cas9 protein<sup>34</sup>. Instead, we identified a  
363 clade of Cas9 in some thermophilic bacteria, and transformed one of these thermostable  
364 ThermoCas9 variants into a powerful genome engineering tool for both thermophilic and  
365 mesophilic organisms. With this study, we further stretched the potential of the Cas9-based  
366 genome editing technologies and open new possibilities for using Cas9 technologies in novel  
367 applications under harsh conditions or requiring activity over a wide temperature range.

368

## 369 **Methods**

### 370 **Bacterial strains and growth conditions**

371 The moderate thermophile *B. smithii* ET 138  $\Delta sigF \Delta hsdR$ <sup>28</sup> was used for the gene editing  
372 and silencing experiments using ThermoCas9. It was grown in LB2 medium<sup>43</sup> at  $55^{\circ}\text{C}$ . For  
373 plates, 30 g of agar (Difco) per liter of medium was used in all experiments. If needed

374 chloramphenicol was added at the concentration of 7  $\mu\text{g/mL}$ . For protein expression, *E. coli*  
375 Rosetta (DE3) was grown in LB medium in flasks at 37°C in a shaker incubator at 120 rpm  
376 until an OD<sub>600 nm</sub> of 0.5 was reached after the temperature was switched to 16°C. After 30 min,  
377 expression was induced by addition of isopropyl-1-thio- $\beta$ -D-gal-actopyranoside (IPTG) to a  
378 final concentration of 0.5 mM, after which incubation was continued at 16°C. For cloning PAM  
379 constructs for 6<sup>th</sup> and 7<sup>th</sup>, and 8<sup>th</sup> positions, DH5a competent *E. coli* (NEB) was transformed  
380 according to the manual provided by the manufacturer and grown overnight on LB agar plates  
381 at 37°C. For cloning degenerate 7-nt long PAM library, electro-competent DH10B *E. coli* cells  
382 were transformed according to standard procedures<sup>52</sup> and grown on LB agar plates at 37°C  
383 overnight. *E. coli* DH5 $\alpha$  *λpir* (Invitrogen) was used for *P. putida* plasmid construction  
384 using the transformation procedure described by Ausubel *et al.*<sup>53</sup>. For all *E. coli* strains,  
385 if required chloramphenicol was used in concentrations of 25 mg/L and kanamycin in 50  
386 mg/L. *Pseudomonas putida* KT2440 (DSM 6125) strains were cultured at 37°C in LB medium  
387 unless stated otherwise. If required, kanamycin was added in concentrations of 50 mg/L and 3-  
388 methylbenzoate in a concentration of 3 mM.

### 389 **ThermoCas9 expression and purification**

390 ThermoCas9 was PCR-amplified from the genome of *G. thermodenitrificans* T12, then  
391 cloned and heterologously expressed in *E. coli* Rosetta (DE3) and purified using FPLC by a  
392 combination of Ni<sup>2+</sup>-affinity, ion exchange and gel filtration chromatographic steps. The gene  
393 sequence was inserted into plasmid pML-1B (obtained from the UC Berkeley MacroLab,  
394 Addgene #29653) by ligation-independent cloning using oligonucleotides (Supplementary  
395 Table 2) to generate a protein expression construct encoding the ThermoCas9 polypeptide  
396 sequence (residues 1-1082) fused with an N-terminal tag comprising a hexahistidine sequence  
397 and a Tobacco Etch Virus (TEV) protease cleavage site. To express the catalytically inactive  
398 ThermoCas9 protein (ThermodCas9), the D8A and H582A point mutations were inserted using  
399 PCR and verified by DNA sequencing.

400 The proteins were expressed in *E. coli* Rosetta 2 (DE3) strain. Cultures were grown to an  
401 OD<sub>600nm</sub> of 0.5-0.6. Expression was induced by the addition of IPTG to a final concentration of  
402 0.5 mM and incubation was continued at 16°C overnight. Cells were harvested by  
403 centrifugation and the cell pellet was resuspended in 20 mL of Lysis Buffer (50 mM sodium  
404 phosphate pH 8, 500 mM NaCl, 1 mM DTT, 10 mM imidazole) supplemented with protease  
405 inhibitors (Roche cOmplete, EDTA-free) and lysozyme. Once homogenized, cells were lysed

406 by sonication (Sonoplus, Bandelin) using a using an ultrasonic MS72 microtip probe  
407 (Bandelin), for 5-8 minutes consisting of 2s pulse and 2.5s pause at 30% amplitude and then  
408 centrifuged at  $16,000\times g$  for 1 hour at  $4^{\circ}\text{C}$  to remove insoluble material. The clarified lysate  
409 was filtered through 0.22 micron filters (Mdi membrane technologies) and applied to a nickel  
410 column (Histrap HP, GE Lifesciences), washed and then eluted with 250 mM imidazole.  
411 Fractions containing ThermoCas9 were pooled and dialyzed overnight into the dialysis buffer  
412 (250 mM KCl, 20 mM HEPES/KOH, and 1 mM DTT, pH 8). After dialysis, sample was diluted  
413 1:1 in 10 mM HEPES/KOH pH 8, and loaded on a heparin FF column pre-equilibrated in IEX-  
414 A buffer (150 mM KCl, 20 mM HEPES/KOH pH 8). Column was washed with IEX-A and  
415 then eluted with a gradient of IEX-C (2M KCl, 20 mM HEPES/KOH pH 8). The sample was  
416 concentrated to 700  $\mu\text{L}$  prior to loading on a gel filtration column (HiLoad 16/600 Superdex  
417 200) via FPLC (AKTA Pure). Fractions from gel filtration were analysed by SDS-PAGE;  
418 fractions containing ThermoCas9 were pooled and concentrated to 200  $\mu\text{L}$  (50 mM sodium  
419 phosphate pH 8, 2 mM DTT, 5% glycerol, 500 mM NaCl) and either used directly for  
420 biochemical assays or frozen at  $-80^{\circ}\text{C}$  for storage.

#### 421 ***In vitro* synthesis of sgRNA**

422 The sgRNA module was designed by fusing the predicted crRNA and tracrRNA sequences  
423 with a 5'-GAAA-3' linker. The sgRNA-expressing DNA sequence was put under the  
424 transcriptional control of the T7 promoter. It was synthesized (Baseclear, Leiden, The  
425 Netherlands) and provided in the pUC57 backbone. All sgRNAs used in the biochemical  
426 reactions were synthesized using the HiScribe™ T7 High Yield RNA Synthesis Kit (NEB).  
427 PCR fragments coding for sgRNAs, with the T7 sequence on the 5' end, were utilized as  
428 templates for in vitro transcription reaction. T7 transcription was performed for 4 hours. The  
429 sgRNAs were run and excised from urea-PAGE gels and purified using ethanol precipitation.

#### 430 ***In vitro* cleavage assay**

431 *In vitro* cleavage assays were performed with purified recombinant ThermoCas9.  
432 ThermoCas9 protein, the *in vitro* transcribed sgRNA and the DNA substrates (generated using  
433 PCR amplification using primers described in Supplementary Table 2) were incubated  
434 separately (unless otherwise indicated) at the stated temperature for 10 min, followed by  
435 combining the components together and incubating them at the various assay temperatures in a  
436 cleavage buffer (100 mM sodium phosphate buffer (pH=7), 500 mM NaCl, 25 mM  $\text{MgCl}_2$ , 25  
437 (V/V%) glycerol, 5 mM dithiothreitol (DTT)) for 1 hour. Each cleavage reaction contained 160

438 nM of ThermoCas9 protein, 4 nM of substrate DNA, and 150 nM of synthesized sgRNA.  
439 Reactions were stopped by adding 6x loading dye (NEB) and run on 1.5% agarose gels. Gels  
440 were stained with SYBR safe DNA stain (Life Technologies) and imaged with a Gel Doc™  
441 EZ gel imaging system (Bio-rad).

#### 442 **Library construction for *in vitro* PAM screen**

443 For the construction of the PAM library, a 122-bp long DNA fragment, containing the  
444 protospacer and a 7-bp long degenerate sequence at its 3'-end, was constructed by primer  
445 annealing and Klenow fragment (exo-) (NEB) based extension. The PAM-library fragment and  
446 the pNW33n vector were digested by BspHI and BamHI (NEB) and then ligated (T4 ligase,  
447 NEB). The ligation mixture was transformed into electro-competent *E. coli* DH10B cells and  
448 plasmids were isolated from liquid cultures. For the 7nt-long PAM determination process, the  
449 plasmid library was linearized by SapI (NEB) and used as the target. For the rest of the assays  
450 the DNA substrates were linearized by PCR amplification.

#### 451 **PAM screening assay**

452 The PAM screening of thermoCas9 was performed using *in vitro* cleavage assays, which  
453 consisted of (per reaction): 160 nM of ThermoCas9, 150 nM *in vitro* transcribed sgRNA, 4 nM  
454 of DNA target, 4 µl of cleavage buffer (100 mM sodium phosphate buffer pH 7.5, 500 mM  
455 NaCl, 5 mM DTT, 25% glycerol) and MQ water up to 20 µl final reaction volume. The PAM  
456 containing cleavage fragments from the 55°C reactions were gel purified, ligated with Illumina  
457 sequencing adaptors and sent for Illumina HiSeq 2500 sequencing (Baseclear). Equimolar  
458 amount of non-ThermoCas9 treated PAM library was subjected to the same process and sent  
459 for Illumina HiSeq 2500 sequencing as a reference. HiSeq reads with perfect sequence match  
460 to the reference sequence were selected for further analysis. From the selected reads, those  
461 present more than 1000 times in the ThermoCas9 treated library and at least 10 times more in  
462 the ThermoCas9 treated library compared to the control library were employed for WebLogo  
463 analysis<sup>54</sup>.

#### 464 ***B. smithii* and *P. putida* editing and silencing constructs**

465 All the primers and plasmids used for plasmid construction were designed with appropriate  
466 overhangs for performing NEBuilder HiFi DNA assembly (NEB), and they are listed in  
467 Supplementary Table 2 and 3 respectively. The fragments for assembling the plasmids were  
468 obtained through PCR with Q5 Polymerase (NEB) or Phusion Flash High-Fidelity PCR  
469 Master Mix (ThermoFisher Scientific), the PCR products were subjected to 1% agarose gel

470 electrophoresis and they were purified using Zymogen gel DNA recovery kit (Zymo Research).  
471 The assembled plasmids were transformed to chemically competent *E. coli* DH5 $\alpha$  cells (NEB),  
472 or to *E. coli* DH5 $\alpha$   $\lambda$ pir (Invitrogen) in the case of *P. putida* constructs, the latter to  
473 facilitate direct vector integration. Single colonies were inoculated in LB medium, plasmid  
474 material was isolated using the GeneJet plasmid miniprep kit (ThermoFisher Scientific) and  
475 sequence verified (GATC-biotech) and 1  $\mu$ g of each construct transformed of *B. smithii* ET 138  
476 electro-competent cells, which were prepared according to a previously described protocol <sup>43</sup>.  
477 The MasterPure™ Gram Positive DNA Purification Kit (Epicentre) was used for genomic DNA  
478 isolation from *B. smithii* and *P. putida* liquid cultures. For the construction of the  
479 pThermoCas9\_ctrl, pThermoCas9\_bs $\Delta$ pyrF1 and pThermoCas9\_bs $\Delta$ pyrF2 vectors, the  
480 pNW33n backbone together with the  $\Delta$ pyrF homologous recombination flanks were PCR  
481 amplified from the pWUR\_Cas9sp1\_hr vector<sup>28</sup> (BG8191 and BG8192). The native P<sub>xyIA</sub>  
482 promoter was PCR amplified from the genome of *B. smithii* ET 138 (BG8194 and BG8195).  
483 The *thermocas9* gene was PCR amplified from the genome of *G. thermodenitrificans* T12  
484 (BG8196 and BG8197). The P<sub>pta</sub> promoter was PCR amplified from the pWUR\_Cas9sp1\_hr  
485 vector <sup>28</sup> (BG8198 and BG8261\_2/BG8263\_nc2/ BG8317\_3). The spacers followed by the  
486 sgRNA scaffold were PCR amplified from the pUC57\_T7t12sgRNA vector  
487 (BG8266\_2/BG8268\_nc2/8320\_3 and BG8210).

488 A four-fragment assembly was designed and executed for the construction of the  
489 pThermoCas9i\_ldhL vectors. Initially, targeted point mutations were introduced to the codons  
490 of the *thermocas9* catalytic residues (mutations D8A and H582A), through a two-step PCR  
491 approach using pThermoCas9\_ctrl as template. During the first PCR step (BG9075, BG9076),  
492 the desired mutations were introduced at the ends of the produced PCR fragment and during  
493 the second step (BG9091, BG9092) the produced fragment was employed as PCR template for  
494 the introduction of appropriate assembly-overhangs. The part of the *thermocas9* downstream  
495 the second mutation along with the *ldhL* silencing spacer was PCR amplified using  
496 pThermoCas9\_ctrl as template (BG9077 and BG9267). The sgRNA scaffold together with the  
497 pNW33n backbone was PCR amplified using pThermoCas9\_ctrl as template (BG9263 and  
498 BG9088). The promoter together with the part of the *thermocas9* upstream the first mutation  
499 was PCR amplified using pThermoCas9\_ctrl as template (BG9089, BG9090)

500 A two-fragment assembly was designed and executed for the construction of  
501 pThermoCas9i\_ctrl vector. The spacer sequence in the pThermoCas9i\_ldhL vector was  
502 replaced with a random sequence containing BaeI restriction sites at both ends. The sgRNA



503 scaffold together with the pNW33n backbone was PCR amplified using pThermoCas9\_ctrl as  
504 template (BG9548, BG9601). The other half of the construct consisting of *thermodcas9* and  
505 promoter was amplified using pThermoCas9i\_ldhL as template (BG9600, BG9549).

506 A five-fragment assembly was designed and executed for the construction of the *P. putida*  
507 KT2440 vector pThermoCas9\_ppΔpyrF. The replicon from the suicide vector pEMG was PCR  
508 amplified (BG2365, BG2366). The flanking regions of *pyrF* were amplified from KT2440  
509 genomic DNA (BG2367, BG2368 for the 576-bp upstream flank, and BG2369, BG2370  
510 for the 540-bp downstream flank). The flanks were fused in an overlap extension PCR  
511 using primers BG2367 and BG2370 making use of the overlaps of primers BG2368 and  
512 BG2369. The sgRNA was amplified from the pThermoCas9\_ctrl plasmid (BG2371,  
513 BG2372). The constitutive P3 promoter was amplified from pSW\_I-SceI (BG2373,  
514 BG2374). This promoter fragment was fused to the sgRNA fragment in an overlap  
515 extension PCR using primers BG2372 and BG2373 making use of the overlaps of primers  
516 BG2371 and BG2374. ThermoCas9 was amplified from the pThermoCas9\_ctrl plasmid  
517 (BG2375, BG2376). The inducible Pm-XylS system, to be used for 3-methylbenzoate  
518 induction of ThermoCas9 was amplified from pSW\_I-SceI (BG2377, BG2378).

### 519 **Editing protocol for *P. putida***

520 Transformation of the plasmid to *P. putida* was performed according to Choi *et al.*<sup>55</sup>.  
521 After transformation and selection of integrants, overnight cultures were inoculated. 10 µl of  
522 overnight culture was used for inoculation of 3 ml fresh selective medium and after 2 hours of  
523 growth at 37°C ThermoCas9 was induced with 3-methylbenzoate. After an additional 6h,  
524 dilutions of the culture were plated on non-selective medium supplemented with 3-  
525 methylbenzoate. For the control culture the addition of 3-methylbenzoate was omitted in all the  
526 steps. Confirmation of plasmid integration in the *P. putida* chromosome was done by colony  
527 PCR with primers BG2381 and BG2135. Confirmation of *pyrF* deletion was done by colony  
528 PCR with primers BG2381 and BG2382.

### 529 **RNA isolation**

530 RNA isolation was performed by the phenol extraction based on a previously described  
531 protocol<sup>56</sup>. Overnight 10 mL cultures were centrifuged at 4°C and 4816×g for 15 min and  
532 immediately used for RNA isolation. After removal of the medium, cells were suspended in 0.5  
533 mL of ice-cold TE buffer (pH 8.0) and kept on ice. All samples were divided into two 2 mL  
534 screw-capped tubes containing 0.5 g of zirconium beads, 30 µL of 10% SDS, 30 µL of 3 M

535 sodium acetate (pH 5.2), and 500  $\mu$ L of Roti-Phenol (pH 4.5–5.0, Carl Roth GmbH). Cells were  
536 disrupted using a FastPrep-24 apparatus (MP Biomedicals) at 5500 rpm for 45 s and centrifuged  
537 at 4°C and 10 000 rpm for 5 min. 400  $\mu$ L of the water phase from each tube was transferred to  
538 a new tube, to which 400  $\mu$ L of chloroform–isoamyl alcohol (Carl Roth GmbH) was added,  
539 after which samples were centrifuged at 4 °C and 18 400 $\times g$  for 3 min. 300  $\mu$ L of the aqueous  
540 phase was transferred to a new tube and mixed with 300  $\mu$ L of the lysis buffer from the high  
541 pure RNA isolation kit (Roche). Subsequently, the rest of the procedure from this kit was  
542 performed according to the manufacturer’s protocol, except for the DNase incubation step,  
543 which was performed for 45 min. The concentration and integrity of cDNA was determined  
544 using Nanodrop-1000 Integrity and concentration of the isolated RNA was checked on a  
545 NanoDrop 1000.

#### 546 **Quantification of mRNA by RT-qPCR**

547 First-strand cDNA synthesis was performed for the isolated RNA using SuperScript™ III  
548 Reverse Transcriptase (Invitrogen) according to manufacturer’s protocol. qPCR was performed  
549 using the PerfeCTa SYBR Green Supermix for iQ from Quanta Biosciences. 40 ng of each  
550 cDNA library was used as the template for qPCR. Two sets of primers were used;  
551 BG9665:BG9666 amplifying a 150-nt long region of the *ldhL* gene and BG9889:BG9890  
552 amplifying a 150-nt long sequence of the *rpoD* (RNA polymerase sigma factor) gene which  
553 was used as the control for the qPCR. The qPCR was run on a Bio-Rad C1000 Thermal Cycler.

#### 554 **HPLC**

555 A high-pressure liquid chromatography (HPLC) system ICS-5000 was used for lactate  
556 quantification. The system was operated with Aminex HPX 87H column from Bio-Rad  
557 Laboratories and equipped with a UV1000 detector operating on 210 nm and a RI-150 40°C  
558 refractive index detector. The mobile phase consisted of 0.16 N H<sub>2</sub>SO<sub>4</sub> and the column was  
559 operated at 0.8 mL/min. All samples were diluted 4:1 with 10 mM DMSO in 0.01 N H<sub>2</sub>SO<sub>4</sub>.

## 560 References

- 561 1. Brouns, S. J. J. *et al.* Small CRISPR RNAs guide antiviral defense in prokaryotes.  
562 *Science* (80-. ). **321**, (2008).
- 563 2. Barrangou, R. *et al.* CRISPR provides acquired resistance against viruses in  
564 prokaryotes. *Science* (80-. ). **315**, (2007).
- 565 3. Wright, A., Nunez, J. & Doudna, J. Biology and applications of CRISPR systems:  
566 Harnessing nature’s toolbox for genome engineering. *Cell* **164**, 29–44 (2016).
- 567 4. Mohanraju, P. *et al.* Diverse evolutionary roots and mechanistic variations of the  
568 CRISPR-Cas systems. *Science* (80-. ). **353**, aad5147 (2016).
- 569 5. Makarova, K. S. *et al.* An updated evolutionary classification of CRISPR–Cas systems.  
570 *Nat. Rev. Microbiol.* **13**, 722–736 (2015).
- 571 6. Komor, A. C. *et al.* CRISPR-based technologies for the manipulation of eukaryotic  
572 genomes. *Cell* **168**, 20–36 (2017).
- 573 7. Puchta, H. Applying CRISPR/Cas for genome engineering in plants: the best is yet to  
574 come. *Curr. Opin. Plant Biol.* **36**, 1–8 (2017).
- 575 8. Xu, J. *et al.* A toolkit of CRISPR-based genome editing systems in *Drosophila*. *J.*  
576 *Genet. Genomics* **42**, 141–149 (2015).
- 577 9. Tang, X. *et al.* A CRISPR–Cpf1 system for efficient genome editing and transcriptional  
578 repression in plants. *Nat. Plants* **3**, 17018 (2017).
- 579 10. Zetsche, B. *et al.* Multiplex gene editing by CRISPR–Cpf1 using a single crRNA array.  
580 *Nat. Biotechnol.* **35**, 31–34 (2016).
- 581 11. Mougiakos, I., Bosma, E. F., de Vos, W. M., van Kranenburg, R. & van der Oost, J.  
582 Next generation prokaryotic engineering: The CRISPR-Cas toolkit. *Trends Biotechnol.*  
583 **34**, 575–587 (2016).
- 584 12. Yan, M.-Y. *et al.* CRISPR-Cas12a-assisted recombineering in bacteria. *Appl. Environ.*  
585 *Microbiol.* AEM.00947-17 (2017). doi:10.1128/AEM.00947-17
- 586 13. Jiang, Y. *et al.* CRISPR–Cpf1 assisted genome editing of *Corynebacterium*  
587 *glutamicum*. *Nat. Commun.* **8**, 15179 (2017).
- 588 14. Jinek, M. *et al.* A programmable dual-RNA-guided DNA endonuclease in adaptive  
589 bacterial immunity. *Science* (80-. ). **337**, 816–821 (2012).
- 590 15. Mojica, F. J. M. Short motif sequences determine the targets of the prokaryotic  
591 CRISPR defence system. *Microbiology* **155**, 733–740 (2009).
- 592 16. Deveau, H. *et al.* Phage response to CRISPR-encoded resistance in *Streptococcus*  
593 *thermophilus*. *J. Bacteriol.* **190**, 1390–400 (2008).
- 594 17. Karvelis, T. *et al.* Rapid characterization of CRISPR–Cas9 protospacer adjacent motif  
595 sequence elements. *Genome Biol.* **16**, 253 (2015).
- 596 18. Bikard, D. *et al.* Programmable repression and activation of bacterial gene expression  
597 using an engineered CRISPR–Cas system. *Nucleic Acids Res.* **41**, 7429–7437 (2013).
- 598 19. Qi, L. S. *et al.* Repurposing CRISPR as an RNA-guided platform for sequence-specific  
599 control of gene expression. *Cell* **152**, 1173–1183 (2013).
- 600 20. Gasiunas, G., Barrangou, R., Horvath, P. & Siksnys, V. Cas9-crRNA ribonucleoprotein  
601 complex mediates specific DNA cleavage for adaptive immunity in bacteria. *Proc.*  
602 *Natl. Acad. Sci. U. S. A.* **109**, E2579-86 (2012).
- 603 21. Lv, L., Ren, Y.-L., Chen, J.-C., Wu, Q. & Chen, G.-Q. Application of CRISPRi for  
604 prokaryotic metabolic engineering involving multiple genes, a case study: Controllable  
605 P(3HB-co-4HB) biosynthesis. *Metab. Eng.* **29**, 160–168 (2015).
- 606 22. Choudhary, E., Thakur, P., Pareek, M., Agarwal, N. & Rajagopalan, M. Gene silencing  
607 by CRISPR interference in mycobacteria. *Nat. Commun.* **6**, 6267 (2015).
- 608 23. Nakade, S., Yamamoto, T. & Sakuma, T. Cas9, Cpf1 and C2c1/2/3—What’s next?

- 609 *Bioengineered* 1–9 (2017). doi:10.1080/21655979.2017.1282018
- 610 24. Bosma, E. F., van der Oost, J., de Vos, W. M. & van Kranenburg, R. Sustainable  
611 production of bio-based chemicals by extremophiles. *Curr. Biotechnol.* **2**, 360–379  
612 (2013).
- 613 25. Taylor, M. P., van Zyl, L., Tuffin, I. M., Leak, D. J. & Cowan, D. A. Genetic tool  
614 development underpins recent advances in thermophilic whole-cell biocatalysts.  
615 *Microb. Biotechnol.* **4**, 438–448 (2011).
- 616 26. Olson, D. G., Sparling, R. & Lynd, L. R. Ethanol production by engineered  
617 thermophiles. *Curr. Opin. Biotechnol.* **33**, 130–141 (2015).
- 618 27. Zeldes, B. M. *et al.* Extremely thermophilic microorganisms as metabolic engineering  
619 platforms for production of fuels and industrial chemicals. *Front. Microbiol.* **6**, 1209  
620 (2015).
- 621 28. Mouggiakos, I. *et al.* Efficient genome editing of a facultative thermophile using  
622 mesophilic spCas9. *ACS Synth. Biol.* **6**, 849–861 (2017).
- 623 29. Wiktor, J., Lesterlin, C., Sherratt, D. J. & Dekker, C. CRISPR-mediated control of the  
624 bacterial initiation of replication. *Nucleic Acids Res.* **44**, 3801–10 (2016).
- 625 30. Daas, M. J. A., van de Weijer, A. H. P., de Vos, W. M., van der Oost, J. & van  
626 Kranenburg, R. Isolation of a genetically accessible thermophilic xylan degrading  
627 bacterium from compost. *Biotechnol. Biofuels* **9**, 210 (2016).
- 628 31. Bosma, E. F. *et al.* Isolation and screening of thermophilic bacilli from compost for  
629 electrotransformation and fermentation: Characterization of *Bacillus smithii* ET 138 as  
630 a new biocatalyst. *Appl. Environ. Microbiol.* **81**, 1874–1883 (2015).
- 631 32. Aparicio, T., Jensen, S. I., Nielsen, A. T., de Lorenzo, V. & Martínez-García, E. The  
632 Ssr protein (T1E\_1405) from *Pseudomonas putida* DOT-T1E enables oligonucleotide-  
633 based recombineering in platform strain *P. putida* EM42. *Biotechnol. J.* **11**, 1309–1319  
634 (2016).
- 635 33. Martínez-García, E. & de Lorenzo, V. The quest for the minimal bacterial genome.  
636 *Curr. Opin. Biotechnol.* **42**, 216–224 (2016).
- 637 34. Li, Y. *et al.* Harnessing Type I and Type III CRISPR-Cas systems for genome editing.  
638 *Nucleic Acids Res.* **44**, e34–e34 (2016).
- 639 35. Ran, F. A. *et al.* In vivo genome editing using *Staphylococcus aureus* Cas9. *Nature*  
640 **520**, 186–191 (2015).
- 641 36. Biswas, A., Gagnon, J. N., Brouns, S. J. J., Fineran, P. C. & Brown, C. M.  
642 CRISPRTarget: bioinformatic prediction and analysis of crRNA targets. *RNA Biol.* **10**,  
643 817–827 (2013).
- 644 37. Kim, S., Kim, D., Cho, S. W., Kim, J. & Kim, J.-S. Highly efficient RNA-guided  
645 genome editing in human cells via delivery of purified Cas9 ribonucleoproteins.  
646 *Genome Res.* **24**, 1012–9 (2014).
- 647 38. Chen, H., Choi, J. & Bailey, S. Cut site selection by the two nuclease domains of the  
648 Cas9 RNA-guided endonuclease. *J. Biol. Chem.* **289**, 13284–13294 (2014).
- 649 39. Zhang, Y., Rajan, R., Seifert, H. S., Mondragon, A. & Sontheimer, E. J. DNase H  
650 Activity of *Neisseria meningitidis* Cas9. *Mol. Cell* **60**, 242–255 (2015).
- 651 40. Ma, E., Harrington, L. B., O’Connell, M. R., Zhou, K. & Doudna, J. A. Single-  
652 Stranded DNA Cleavage by Divergent CRISPR-Cas9 Enzymes. *Mol. Cell* **60**, 398–407  
653 (2015).
- 654 41. Bhalla, A., Bansal, N., Kumar, S., Bischoff, K. M. & Sani, R. K. Improved  
655 lignocellulose conversion to biofuels with thermophilic bacteria and thermostable  
656 enzymes. *Bioresour. Technol.* **128**, 751–759 (2013).
- 657 42. Abdel-Banat, B. M. A., Hoshida, H., Ano, A., Nonklang, S. & Akada, R. High-  
658 temperature fermentation: how can processes for ethanol production at high

- 659 temperatures become superior to the traditional process using mesophilic yeast? *Appl.*  
660 *Microbiol. Biotechnol.* **85**, 861–867 (2010).
- 661 43. Bosma, E. F. *et al.* Establishment of markerless gene deletion tools in thermophilic  
662 *Bacillus smithii* and construction of multiple mutant strains. *Microb. Cell Fact.* **14**, 99  
663 (2015).
- 664 44. Oh, J.-H. & van Pijkeren, J.-P. CRISPR-Cas9-assisted recombineering in *Lactobacillus*  
665 *reuteri*. *Nucleic Acids Res.* **42**, e131 (2014).
- 666 45. Nikel, P. I., Chavarría, M., Danchin, A. & de Lorenzo, V. From dirt to industrial  
667 applications: *Pseudomonas putida* as a Synthetic Biology chassis for hosting harsh  
668 biochemical reactions. *Curr. Opin. Chem. Biol.* **34**, 20–29 (2016).
- 669 46. Poblete-Castro, I., Becker, J., Dohnt, K., dos Santos, V. M. & Wittmann, C. Industrial  
670 biotechnology of *Pseudomonas putida* and related species. *Appl. Microbiol. Biotechnol.*  
671 **93**, 2279–2290 (2012).
- 672 47. Larson, M. H. *et al.* CRISPR interference (CRISPRi) for sequence-specific control of  
673 gene expression. *Nat. Protoc.* **8**, 2180–2196 (2013).
- 674 48. Weinberger, A. D., Wolf, Y. I., Lobkovsky, A. E., Gilmore, M. S. & Koonin, E. V.  
675 Viral diversity threshold for adaptive immunity in prokaryotes. *MBio* **3**, e00456-12  
676 (2012).
- 677 49. Jinek, M. *et al.* Structures of Cas9 endonucleases reveal RNA-mediated conformational  
678 activation. *Science (80-. )*. **343**, 1247997–1247997 (2014).
- 679 50. Kelley, L. A., Mezulis, S., Yates, C. M., Wass, M. N. & Sternberg, M. J. E. The Phyre2  
680 web portal for protein modeling, prediction and analysis. *Nat. Protoc.* **10**, 845–858  
681 (2015).
- 682 51. Kumar, S., Stecher, G. & Tamura, K. MEGA7: Molecular evolutionary genetics  
683 analysis version 7.0 for bigger datasets. *Mol. Biol. Evol.* **33**, 1870–1874 (2016).
- 684 52. Sambrook, J., Fritsch, E. F. & Maniatis, T. *Molecular cloning : a laboratory manual*.  
685 (Cold Spring Harbor Laboratory, 1989).
- 686 53. *Current Protocols in Molecular Biology*. (John Wiley & Sons, Inc., 2001).  
687 doi:10.1002/0471142727
- 688 54. Crooks, G. E., Hon, G., Chandonia, J.-M. & Brenner, S. E. WebLogo: A sequence logo  
689 generator. *Genome Res.* **14**, 1188–1190 (2004).
- 690 55. Choi, K.-H., Kumar, A. & Schweizer, H. P. A 10-min method for preparation of highly  
691 electrocompetent *Pseudomonas aeruginosa* cells: Application for DNA fragment  
692 transfer between chromosomes and plasmid transformation. *J. Microbiol. Methods* **64**,  
693 391–397 (2006).
- 694 56. van Hijum, S. A. F. T. *et al.* A generally applicable validation scheme for the  
695 assessment of factors involved in reproducibility and quality of DNA-microarray data.  
696 *BMC Genomics* **6**, 77 (2005).

698

699

700

701

702

703 **Acknowledgements**

704 We would like to thank Koen Weenink, Steven Aalvink and Bastienne Vriesendorp for their  
705 technical assistance. R.v.K. is employed by Corbion. I.M. and E.F.B. are supported by the  
706 Dutch Technology Foundation STW, which is part of The Netherlands Organization for  
707 Scientific Research (NWO) and which is partly funded by the Ministry of Economic Affairs.  
708 J.v.d.O. and P.M. are supported by the NWO/TOP grant 714.015.001. R.B. is financially  
709 supported by Corbion. A patent application has been filed related to this work.

710

711 **Author contributions**

712 I.M., P.M., E.F.B., R.v.K., and J.v.d.O., conceived this study and design of experiments. I.M.,  
713 P.M., E.F.B., M.F., V.V., M.N., A.G., and R.B. conducted the experiments. R.v.K. and J.v.d.O.  
714 supervised this project. I.M., P.M., E.F.B., R.v.K., and J.v.d.O. wrote the manuscript with input  
715 from all authors.

716

717 **Competing interests**

718 The authors declare no competing financial interests.

719

720 **Data availability**

721 Plasmids expressing ThermoCas9 or ThermodCas9, together with the corresponding sgRNA,  
722 are available on Addgene (#tba).

723 **Corresponding author**

724 Correspondence and requests for materials should be addressed to J.v.d.O.  
725 ([john.vanderoost@wur.nl](mailto:john.vanderoost@wur.nl)).

726

727 **Figures**

728

729 **Figure 1. The *Geobacillus thermodenitrificans* T12 type-II CRISPR-Cas locus encodes a**  
730 **thermostable Cas9 homolog, ThermoCas9.**

731 (A) Schematic representation of the genomic locus encoding ThermoCas9. The domain  
732 architecture of ThermoCas9 based on sequence comparison, with predicted active sites  
733 residues highlighted in magenta. A homology model of ThermoCas9 generated using Phyre  
734 2<sup>50</sup> is shown, with different colours for the domains.

735 (B) Phylogenetic tree of Cas9 orthologues those are highly identical to ThermoCas9.  
736 Evolutionary analysis was conducted in MEGA7<sup>51</sup>.

737 (C) SDS-PAGE of ThermoCas9 after purification by metal-affinity chromatography and gel  
738 filtration. The migration of the obtained single band is consistent with the theoretical  
739 molecular weight of 126 kD of the apo-ThermoCas9.

740

741 **Figure 2. ThermoCas9 PAM analysis.**

742 (A) Schematic illustrating the *in vitro* cleavage assay for discovering the position and  
743 identity (5'-NNNNNNN-3') of the protospacer adjacent motif (PAM). Magenta triangles  
744 indicate the cleavage position.

745 (B) Sequence logo of the consensus 7nt long PAM of ThermoCas9, obtained by  
746 comparative analysis of the ThermoCas9-based cleavage of target libraries. Letter height at  
747 each position is measured by information content.

748 (C) Extension of the PAM identity to the 8th position by *in vitro* cleavage assay. Four  
749 linearized plasmid targets, each containing a distinct 5'-CCCCCAN-3 PAM, were incubated  
750 with ThermoCas9 and sgRNA at 55°C for 1 hour, then analysed by agarose gel  
751 electrophoresis.

752 (D) *In vitro* cleavage assays for DNA targets with different PAMs at 30°C and 55°C. Sixteen  
753 linearized plasmid targets, each containing one distinct 5'-CCCCNNA-3' PAM, were  
754 incubated with ThermoCas9 and sgRNA, then analysed for cleavage efficiency by agarose  
755 gel electrophoresis. See also Supplementary Fig. 3.

756

757 **Figure 3. ThermoCas9 is active at a wide temperature range and its thermostability**  
758 **increases when bound to sgRNA.**

759 (A) Schematic representation of the sgRNA and a matching target DNA. The target DNA,  
760 the PAM and the crRNA are shown in grey, blue and green, respectively. The site where the  
761 crRNA is linked with the tracrRNA is shown in purple. The dark blue and light blue boxes  
762 indicate the predicted three and two loops of the tracrRNA, respectively. The 41-nt truncation  
763 of the repeat-antirepeat region and the three loops of the sgRNA are indicated by the magenta  
764 dotted line and magenta triangles, respectively.

765 (B) The importance of the predicted three stem-loops of the tracrRNA scaffold was tested  
766 by transcribing truncated variants of the sgRNA and evaluating their ability to guide  
767 ThermoCas9 to cleave target DNA at various temperatures. Average values of at least two  
768 biological replicates are shown, with error bars representing S.D.

769 (C) To identify the maximum temperature, endonuclease activity of ThermoCas9:sgRNA  
770 RNP complex was assayed after incubation at 60°C, 65°C and 70°C for 5 or 10 min. The pre-  
771 heated DNA substrate was added and the reaction was incubated for 1 hour at the  
772 corresponding temperature.

773 (D) Comparison of active temperature range of ThermoCas9 and SpCas9 by activity assays  
774 conducted after 5 min of incubation at the indicated temperature. The pre-heated DNA  
775 substrate was added and the reaction was incubated for 1 hour at the same temperature.

776

#### 777 **Figure 4. ThermoCas9-based genome engineering in thermophiles.**

778 (A) Schematic overview of the basic pThermoCas9\_Δgene-of-interest (goi) construct. The  
779 *thermocas9* gene was introduced either to the pNW33n (*B. smithii*) or to the pEMG (*P. putida*)  
780 vector. Homologous recombination flanks were introduced upstream *thermocas9* and  
781 encompassed the 1kb (*B. smithii*) or 0.5kb (*P. putida*) upstream and 1kb or 0.5 kb downstream  
782 region of the gene of interest (goi) in the targeted genome. A sgRNA-expressing module was  
783 introduced downstream the *thermocas9* gene. As the origin of replication (ori), replication  
784 protein (rep), antibiotic resistance marker (AB) and possible accessory elements (AE) are  
785 backbone specific, they are represented with dotted outline.

786 (B) Agarose gel electrophoresis showing the resulting products from genome-specific PCR  
787 on ten colonies from the ThermoCas9-based *pyrF* deletion process from the genome of *B.*  
788 *smithii* ET 138. All ten colonies contained the Δ*pyrF* genotype and one colony was a clean  
789 Δ*pyrF* mutant, lacking the wild type product.

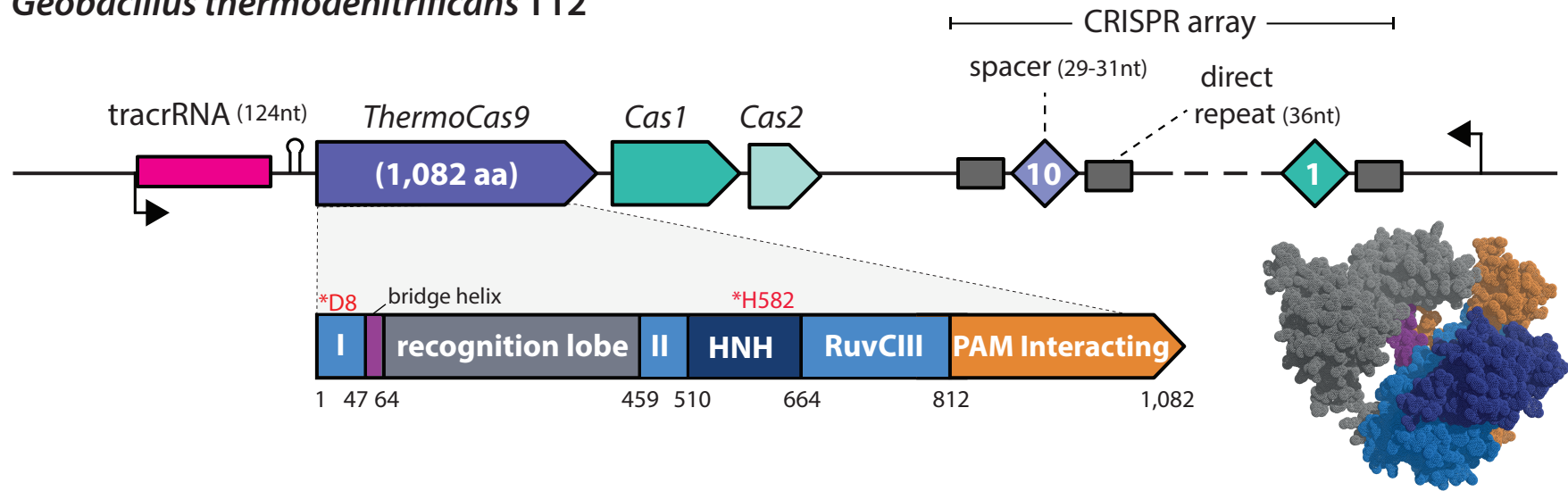


790 (C) Schematic overview of the basic pThermoCas9i\_goi construct. Aiming for the  
791 expression of a catalytically inactive ThermoCas9 (ThermodCas9: D8A, H582A mutant), the  
792 corresponding mutations were introduced to create the *thermodcas9* gene. The *thermodcas9*  
793 gene was introduced to the pNW33n vector. A sgRNA-expressing module was introduced  
794 downstream the *thermodcas9*.

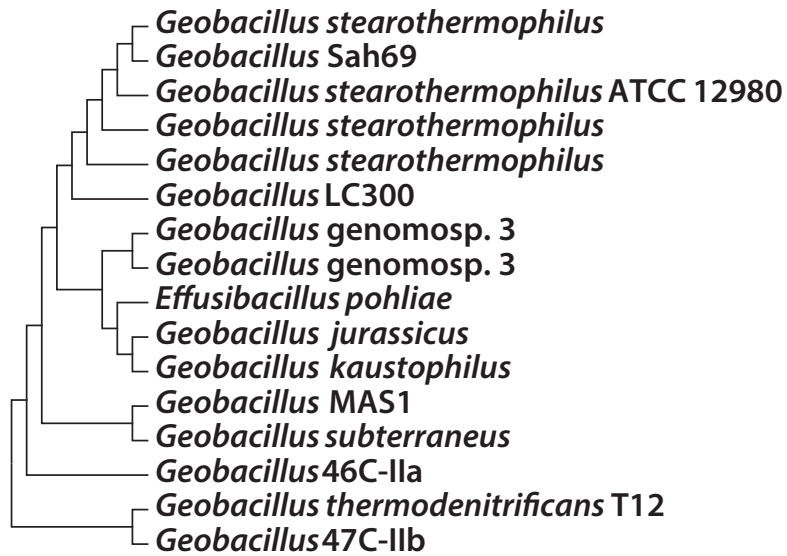
795 (D) Graphical representation of the production, growth and RT-qPCR results from the *ldhL*  
796 silencing experiment using ThermodCas9. The graphs represent the lactate production,  
797 optical density at 600nm and percentage of *ldhL* transcription in the repressed cultures  
798 compared to the control cultures. Average values from at least two biological replicates are  
799 shown, with error bars representing S.D.

a.

## *Geobacillus thermodenitrificans* T12



b.



c.

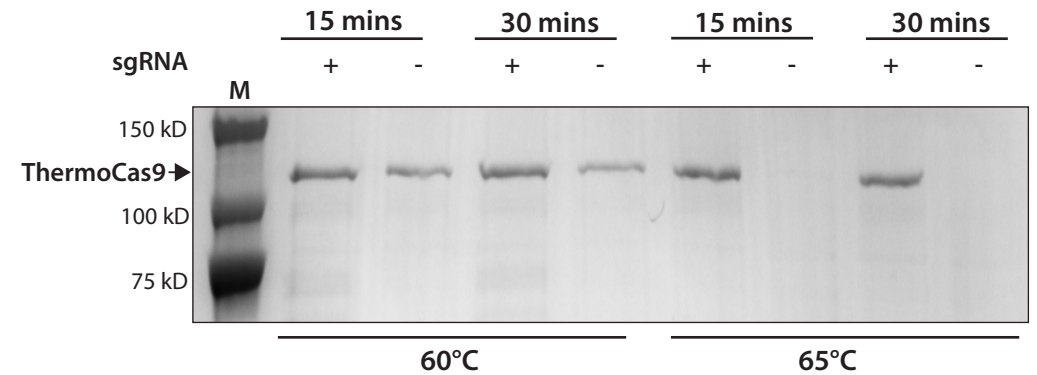
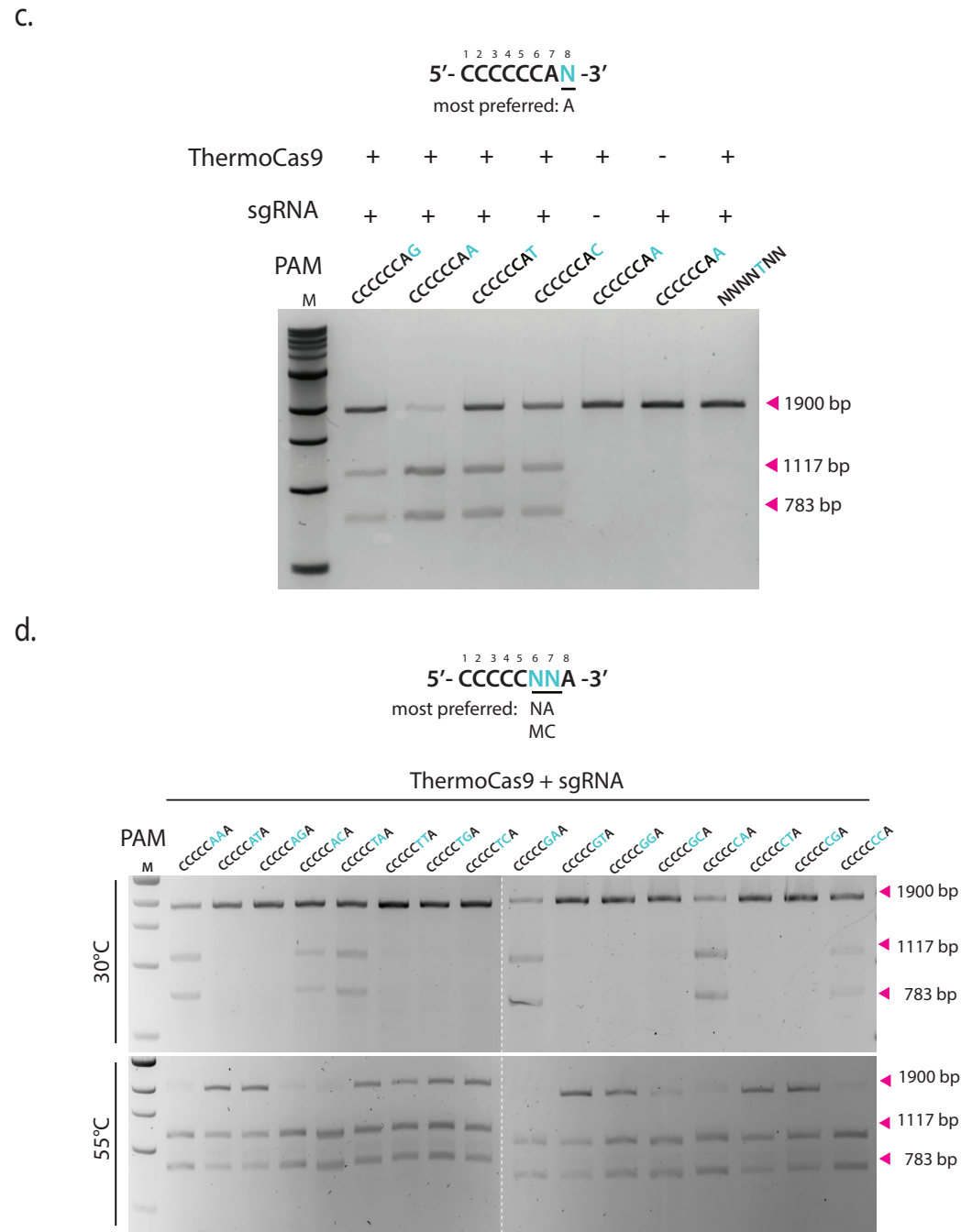
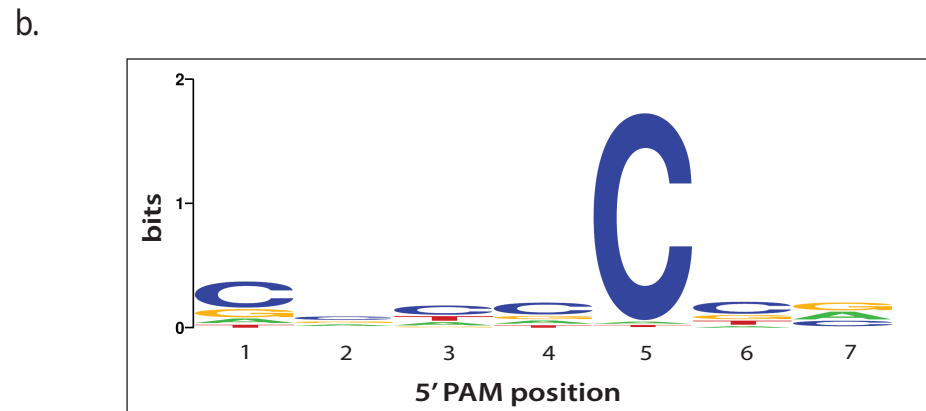


Figure 1



**Figure 2**

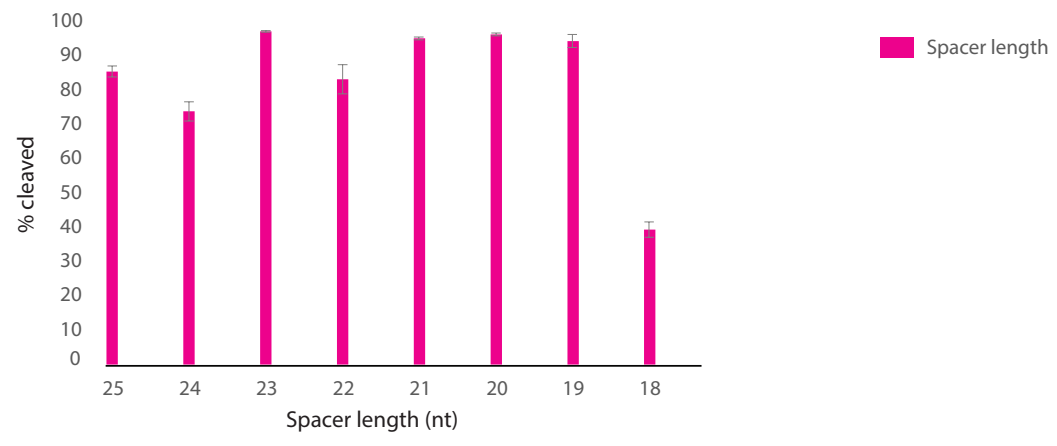
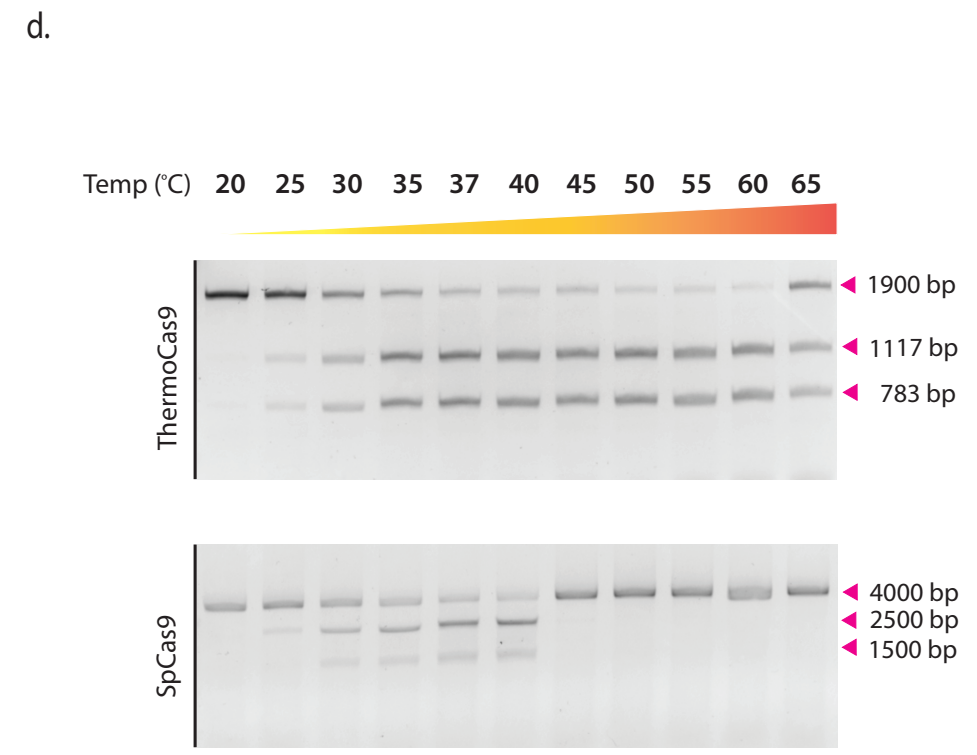
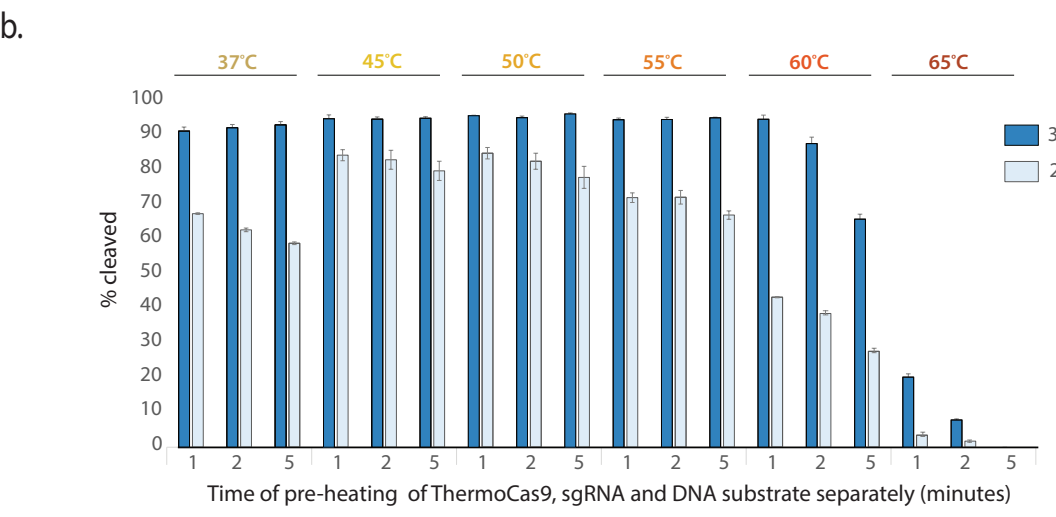
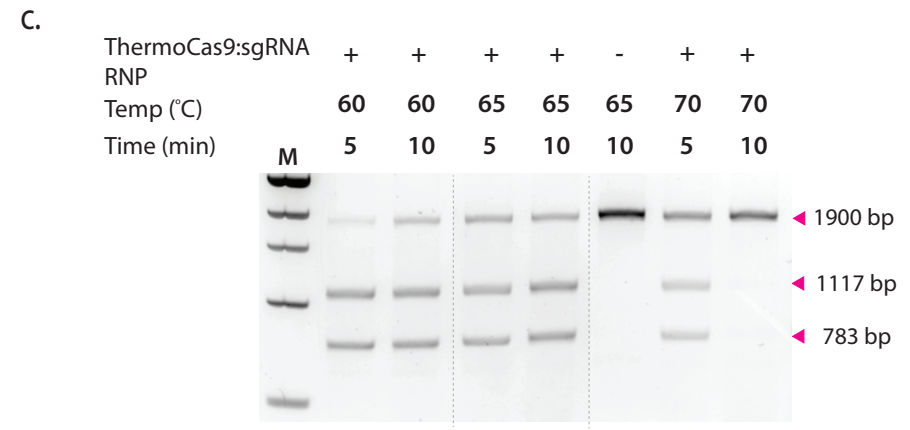
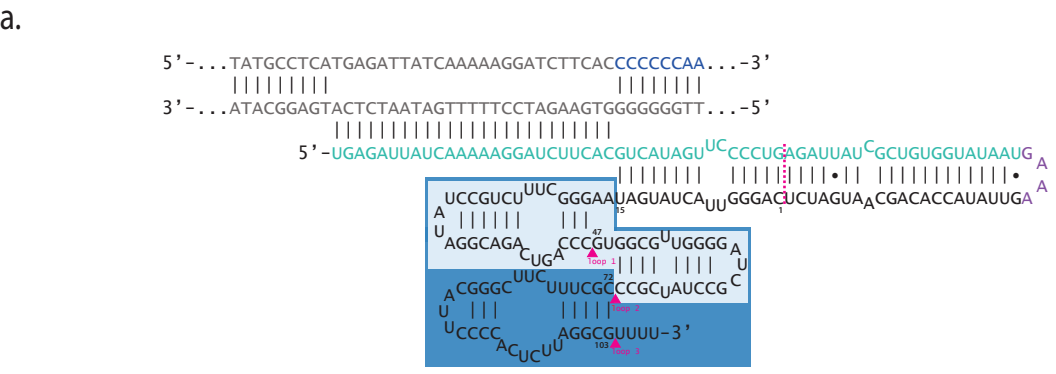


Figure 3

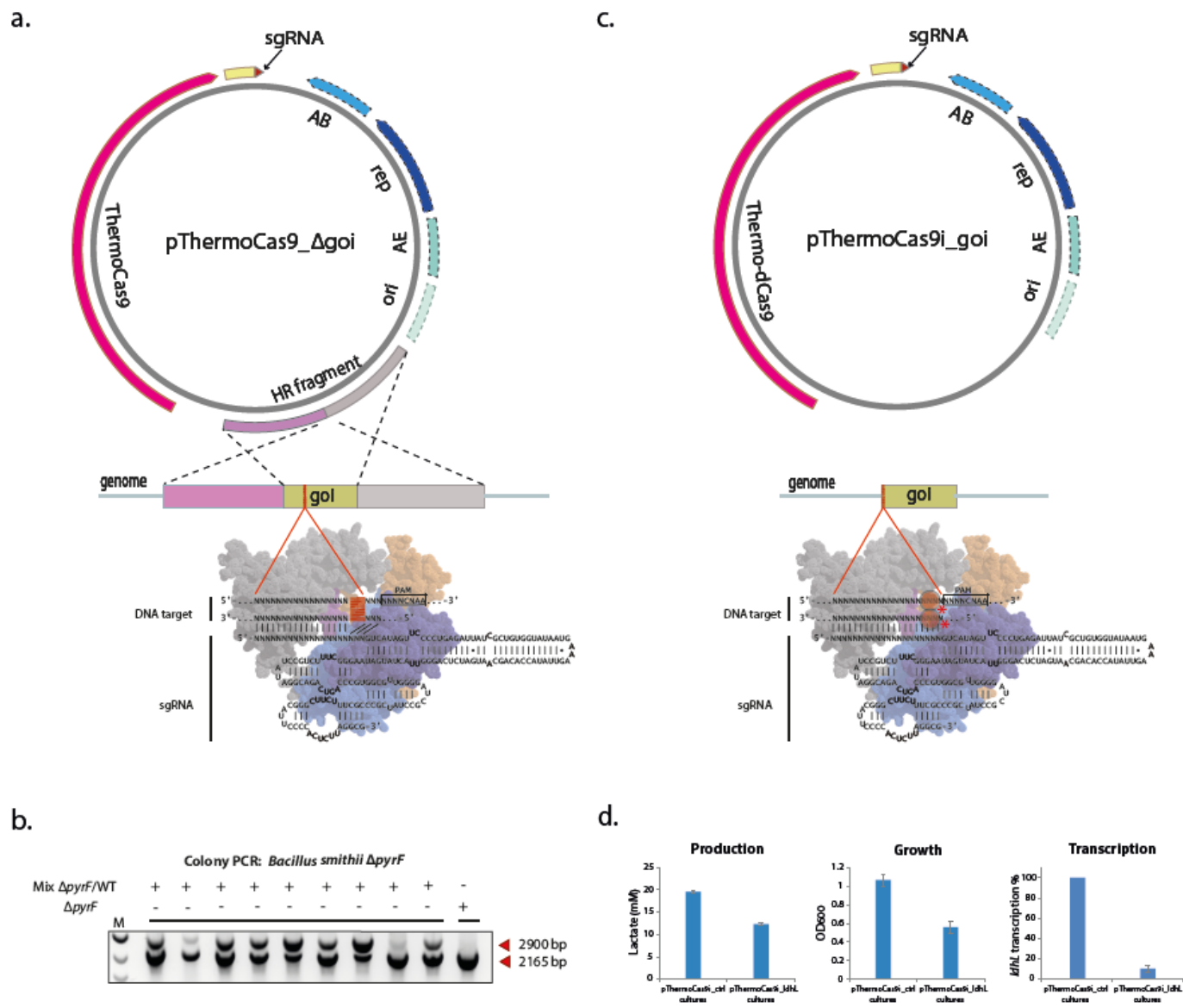


Figure 4